Branching and Higher Order Structure in Banded Polyethylene Spherulites

Akihiko Toda,*,† Mari Okamura,‡ Ken Taguchi,† Masamichi Hikosaka,† and Hiroshi Kajioka§

Graduate School of Integrated Arts and Sciences and Graduate School of Biosphere Science, Hiroshima University, 1-7-1 Kagamiyama, Higashi-Hiroshima 739-8521, Japan, and Graduate School of Science, Kyoto University, Sakyo-ku, Kyoto 606-8521, Japan

Received October 11, 2007; Revised Manuscript Received January 6, 2008

ABSTRACT: Because of twisting correlation of crystallites along the radial direction, polyethylene spherulites are known to develop concentric band pattern. The mechanism of branching and reorientation of lamellar crystallites in the banded spherulites has been examined experimentally by optical and atomic force microscopies associated with quenching and chemical etching. The microscopic observation suggests a branching instability of lamellar crystals at the growth front of the spherulite. We propose a mechanism of consecutive branching and twisting reorientation of branches regulated by the inherent torsional stress expected for the banded spherulites and the branching instability. We have experimentally examined the relationships among the growth rate, the maximum lateral width of crystals at the growth front, and the period of bands for three different molecular weight fractions of polyethylene. The predicted relationship among them holds for the fractions.

Introduction

When polymers crystallize from the melt or from viscous liquids, a higher order structure of crystallites evolves as a spherulite with radiating and space-filling branches of chain-folded lamellar crystallites. A beautiful pattern of concentric rings is developed in a variety of polymer spherulites, and they are called banded (or ringed) spherulites. In the late 19th and early 20th centuries, ringed spherulites of organic crystals have been actively studied.[1] After the recognition of polymer banded spherulites,[2] a number of studies have been made on the mechanism of the structural formation.[3–5]

Pioneering works of Point,[6] Keith and Padden,[7] Price,[8] and Keller[9] have confirmed that the concentric extinction pattern seen by optical microscopy corresponds to the rotation of the optical axis of lamellar crystallites with respect to the radial axis of spherulites. Subsequently, Fujiwara[10] has confirmed the rotation of the crystal axis by microbeam X-ray diffraction. Those confirmations clearly suggest the twisting correlation of lamellar crystallites along the radial axis in the polymer spherulites having a concentric ring pattern. In order to understand the formation mechanism of the banded polymer spherulites, we think we must clarify (1) the origin of the torsional stress in lamellar crystals, (2) the selection mechanism of ring period, and (3) the mechanism of coordination of twisting correlation along the tangential direction of spherulites.

Concerning the origin of the torsional stress in thin lamellar crystallites with chain folding, it is known that the folding of chains needs larger cross section than crystalline stems,[11] and hence the steric hindrance and the congestion of folds induce stress on the upper and lower surface regions of thin lamellar crystallites. The stress will be anisotropic corresponding to the direction of chain folding and unbalanced due to the molecular structure of folds, so that there will be an anisotropic unbalance of surface stresses due to the fold geometry on the upper and lower surface regions.[12] The typical example will be the scrolled single crystals grown from solution of poly(1-butene) in form III[13,14] and of polyamides[15,16] and the scrolled crystals grown from the melt of poly(vinylidene fluoride) in the γ phase[17,18] and of monodisperse centrally branched alkanes.[19] All those deformations of the lamellar crystals are supposed to be caused by the asymmetry of fold structure on the upper and lower surface regions.[12]

On the other hand, the stress on the folding surfaces can be relaxed by the tilting of crystalline stems with respect to the folding surfaces because of the increase in the cross section of surface regions.[20,21] There are suggestions of the origin of torsional stress introduced by the chain tilting. First, the tilting is supposed to induce different overcrowding in opposite fold surfaces due to the process of reeling-in of polymer chains along the tilted growth front.[22–24] The unbalance of the overcrowding induces torsional stress with one of the senses (e.g., right-handedness) in one of the growth directions of ribbonlike lamellar crystal and another sense (e.g., left-handedness) in the opposite growth direction. Second, the three-dimensional shape of the crystals with chain tilting can be intrinsically strained to be like a chair with the sense of torsion similar to the above.[25–27] Those possibilities with chain tilting will be applicable to nonchiral polymers having twisting correlation of both hands coexisting in a banded spherulite. For nonracemic chiral polymers, on the other hand, possible models will be based on the helix handedness of chiral polymers. Actually, it is known that the handedness of twisting correlation in the banded spherulites is uniquely determined for chiral polymers, though there is no general one-to-one (e.g., right−right) correspondence between the handedness of helix and of twisting correlation.[28] On the basis of the expected differences in the fold conformations of helical chains, there have been suggestions on the origin of the torsional stress in the lamellar crystals of chiral polymers.[12,29] As a final remark on the origin of the torsional stress, it will also be probable that all those factors mentioned in the above become built up on reorganization of folding surfaces with lamellar thickening, as suggested by Bassett et al.[5,30,31] The origin of the twist and scroll geometries of lamellar crystals has recently been intensively reviewed by Lotz and Cheng.[12]

As briefly summarized above, the inherent torsional stress and the consequent twisting correlation should be attributed to the structures at the molecular level of chain conformation and

* Corresponding author: tel +81-82-424-6558, fax +81-82-424-0757, e-mail atoda@hiroshima-u.ac.jp.
† Graduate School of Integrated Arts and Sciences, Hiroshima University.
‡ Graduate School of Biosphere Science, Hiroshima University.
§ Kyoto University.

10.1021/ma702267e CCC: $40.75
Published on Web 02/28/2008

packing. The continuous twist of lamellar crystals has been confirmed by microscopic observations for isolated individual single crystals of polyethylene,[32,33] silk fibroin,[34] nonracemic chiral main-chain polyesters,[35–38] and chiral poly(R-3-hydroxybutyrate-*co*-R-3-hydroxyhexanoate) copolymer.[39] In order to answer the second question on the selection mechanism of ring periodicity in the spherulites formed by the radiating and space-filling branches of lamellar crystallites, the higher order structure of lamellar crystals can be an important factor because the period may not be simply determined by the pitch of the continuous twist of each lamellar crystal. Actually, it has been suggested by Bassett and Hodge[40] for polyethylene crystallization from the melt and by Xu et al.[39] that the twisting is nonuniform and amplified on branching with the formation of giant screw dislocations. The repetitive lamellar twisting and splaying in a banded spherulite of poly(vinylidene fluoride) grown from poly(vinylidene fluoride)/poly(ethyl acrylate) blend have also been reported by Briber and Khoury.[41] In this case, it is important to understand the mechanism of branching and splaying in lamellar crystals. On the other hand, since the branching frequency will determine the lateral width of lamellar crystals at the growth front, branching can also be an important factor for continuous twist in the case that the twist angle is limited by the lateral width, as recently suggested by Muthukumar.[42] The branching and splaying mechanism itself has been a quite important and controversial issue in the discussion of the formation mechanism of polymer spherulites in general with space-filling branches by a noncrystallographic reorientation.[40,43,44]

As the source of branching, Keith and Padden[45] suggested a possibility of morphological instability caused by the diffusion field of noncrystallizing fractions at the growth front of polymer spherulites. Because of the built-up concentration profile of noncrystallizing fractions, there can be a gradient of driving force of crystallization at the growth front. Then, the part of growth front sticking out from the mean position by fluctuations can feel larger driving force, and hence the fluctuation can be accelerated. Because of the instability, they have supposed that the characteristic length of growth front is in proportion to the diffusion length, $\delta = D/V$, which is a measure of the gradient of the diffusion field with the diffusion coefficient, D, and the growth velocity, V. The characteristic length may correspond to the critical width for the branching of lamellar crystals. Experimentally, the lamellar morphology of polyethylene spherulites has been examined by Bassett and Hodge[40] and Keith and Padden[46] and that of nonbanded spherulites of it-polypropylene and it-polystyrene by Bassett and Olley[43] and by Bassett and Vaughan,[44] respectively. The expected relationship between the diffusion length and the width of lamellar crystals was not confirmed, though Keith and Padden[46] reported a consistent change in the characteristic size of a leading entity, such as parallel dominant lamellae and lamellar stacks in parallel orientation. Bassett et al.[40,43,44] have suggested that the important morphological unit is not the fibrous texture supposed by Keith and Padden,[45] but the branching and splaying of individual dominant lamellae.

In terms of the relationship between the diffusion length and the characteristic length formed by the morphological instability, Goldenfeld[47] suggested the stabilizing effect of surface tension. The critical length is then determined by the balance between the destabilizing effect of the gradient of compositional field and the stabilizing effect of surface tension. Then, the characteristic length is not in proportion to δ but depends on the square root of δ on the basis of the theoretical modeling of Mullins and Sekerka.[48,49] Goldenfeld[47] has also suggested that the stationary growth at a constant velocity can be realized for the growth controlled by the diffusion field with the kinetics of crystallization at the growth front. Therefore, the linear growth of polymer spherulites and the branching instability at the growth front can be explained as the growth controlled by the diffusion and the kinetics, instead of the growth only limited by diffusion, which basically results in the movement of the interface with square root of elapsed time.

Figure 1. $1.6 \times 1.6\ \mu m^2$ AFM amplitude image of a polyethylene single crystal grown from the melt. The growth front was split at a certain distance into small branches twisted to form the spiral terraces in the same sense. The split pattern was formed on the course of quenching from isothermal condition at 120 °C to a coolant held at −90 °C. Sample was chemically etched to reveal the single crystal.[62]

In the present paper, on the basis of those detailed discussions on the twisting and branching mechanisms of lamellar crystals in prior studies, we put our focus on the structural formation at the mesoscopic scale of the branching and reorientation of lamellar crystals in the banded spherulites. We will propose a mechanism for the variation of the periodicity of rings by incorporating the spontaneous twist by surface stresses and the branching instability at the growth front of individual crystals. Both of the elements have been discussed in prior research, as described in the above, but the coupling of them has not been considered before. Not only the effect of compositional gradient, we will also consider the possibility of mechanical (pressure) gradient in a viscous liquid,[50,51] which is expected because of necessary flow to balance the density difference between the crystal and the melt; the possibility of the self-induced field of pressure gradient in polymer crystallization has been pointed out by Schultz.[52] The destabilization by the flow seems to be dominant in the crystallization from ultrathin melt.[53] Concerned with the destabilization of growth front of polymer crystals grown from the bulk melt, in our recent observation of melt-crystallized polyethylene, we have found a typical example of tip splitting at the growth front of single crystals grown from the melt (Figure 1). We think that this pattern will be the direct evidence of the branching instability of growth front, and so we think there will also be the branching instability for the spherulitic growth from the bulk melt.

We suppose that the individual lamellar crystal undergoes branching instability at a critical lateral width and reorients the direction by the inherent torsional stress discussed in the above. For the second question of the periodicity of rings, the reorientation of lamellae on the occasion of splaying can be an important factor if the angle of reorientation is the dominant factor for the periodicity. In this case, it will be shown that the ring period is proportional to the lateral width of lamellae. On the other hand, the proportional dependence can also be expected for continuous twist without the dominant effect of reorientation

on splaying if the pitch is limited by the lateral size. So, we will propose a proportional relationship between the ring period and the size of the building blocks, namely the lateral size of lamellae, irrespective of the cause of the relationship. For the third question about the coordination of twisting in the tangential direction, we can expect the correlation between mother and daughter lamellae formed by branching.[54]

We think that the unsuccessful observations of the relationship between the lateral width of lamellar crystals and the diffusion length, δ, in prior studies were partly due to the prediction of the proportional relationship between them, which must be much weaker square root dependence and may have been due to the temperature range for the polyethylene spherulites examined. For the banded spherulites of polyethylene with sharp change in the band spacing with crystallization temperature, the temperature range must be low enough. In the present paper, we examine the growth of polyethylene spherulites in the temperature range where the band spacing changes with temperature by almost one order in magnitude, so that we also expect the change in the lateral width of lamellar crystals in the same order, on the basis of the expected proportional relationship between them. In order to investigate the lower temperature range, we utilize sliding hot cells[55] to apply rapid temperature jump to the crystallization temperature and instantaneous quench to stop the growth for the subsequent examination by microscopy.

In the following, we first propose our modeling based on both the branching instability and the inherent torsional stress in the crystals of banded spherulites. Then, we confirm the predicted relationships of the growth rate, the lateral width of crystals at the growth front, and the periodicity of rings experimentally for polyethylene of three different molecular weight fractions.

Modeling

Branching and Reorientation. Our modeling is based upon the branching instability of growth front and the reorientation of the branches due to inherent torsional stress in the lamellar crystals of banded spherulites. We suppose that the branching instability limits the maximum lateral width, λ, of the individual crystals at the growth front of spherulites; the crystal wider than the critical width becomes unstable and splays into a pair of branches, as shown in Figure 2. Then, the torsional surface stresses of banded spherulites introduce the reorientation of the branches at an angle keeping the handedness in the same manner, so that the branches are physically separated from each other. The angle can be small on the occasion of splaying and may become larger subsequently on reorganization of folding surfaces with lamellar thickening.[5,30,31] Because of the independent growth, the branches can grow in width as well as in length, and the width at the growth front will eventually become larger than the maximum lateral width, λ, again, so that the crystal will undergo branching and splaying repeatedly. By this mechanism, the consecutive branching and twisting reorientation will be repeated at the growth front and will provide the branching frequency high enough to fill in the 3-d space in spherulites with noncrystallographic branching caused by the spontaneous reorientation. It is noted that the process may correspond to the suggestion of the motif of the repetitive lamellar twisting and splaying reported by Briber and Khoury[41] for poly(vinylidene fluoride) banded spherulites. It is also noted that, in this modeling, growth dislocations will be created at the boundary of neighboring branches as the consequence of the physical separation of the twisted branches (Figure 2). The formation of screw dislocation will therefore not be limited by thermal activation process to overcome the strain energy of dislocation.

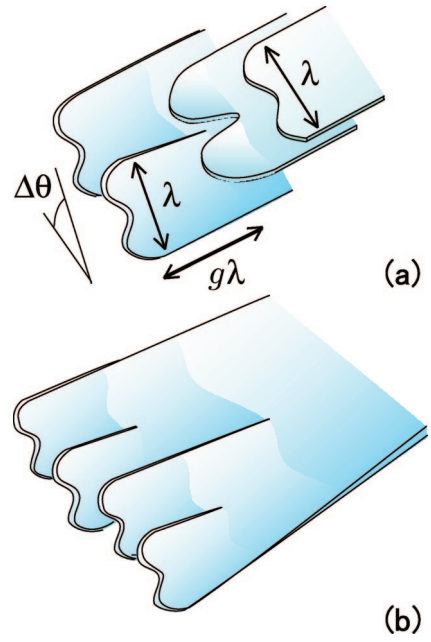

Figure 2. Schematic illustrations of (a) the evolution of crystal branching at the critical width, λ, and the reorientation on splaying and (b) the expected structure.

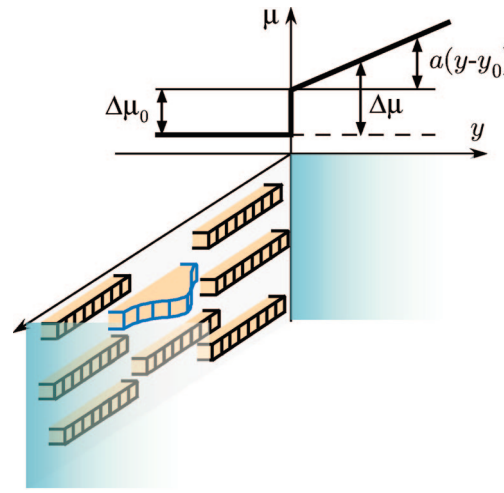

Figure 3. Schematic illustration of possible gradient field spontaneously formed at the growth front of a spherulite by the group of lamellar crystals and the change in chemical potential, μ, due to the gradient.

Branching by a Gradient Field. In the present modeling, we suppose the branching instability caused by a gradient in chemical potential at the growth front of spherulites in the liquid side. For a thin lamellar crystal, the formation of effective gradient field around the individual crystal may be questioned if it is isolated in the liquid. However, at the growth front of a spherulite, the gradient field will be spontaneously formed by the group of lamellar crystals growing in parallel with each other, as shown in Figure 3. Then, each lamellar crystal will feel the gradient field sustained by the group of lamellar stacks and undergoes the branching instability on its own. Actually, recent observations by in-situ SPM of the crystallization appearing on the sample surface suggest the fluctuation of growth rate and the unstable growth front of individual crystals, which eventually evolve branching to form spiral terraces,[39,56] as discussed above.

In our observation of single crystals of polyethylene grown from the melt, we have also noticed quite interesting pattern of the growth front which is split at a certain distance into small

branches being twisted to form the spiral terraces in the same sense (Figure 1). This pattern will be the direct evidence of the branching and splaying of growth front, which has occurred on the course of quenching of the single crystal grown under isothermal condition.

Regarding the possible branching instability caused by a gradient field, the most well-known one will be of Mullins−Sekerka type[48,49] caused by composition or temperature gradient at the growth front in the liquid side. Although the original modeling of Mullins−Sekerka supposes the growth only limited by diffusion, the modeling is also applicable to the growth controlled both by the diffusion and by the surface kinetics, as suggested by Goldenfeld.[47] Therefore, the linear growth controlled by both factors and the branching instability of the interface are predicted from the modeling.[47]

For polymer crystallization, it is known that the thermal diffusion length, which is determined by the thermal diffusion coefficient and the growth rate, becomes much larger than the size of spherulites, and hence the growth face is supposed to be stable against the weak temperature gradient. On the other hand, synthetic polymers inevitably have common characteristics of multicomponent systems with molecular weight distribution and defects in the chain structure, both of which introduce the distribution of melting temperatures and hence of supercoolings. Actually, it has been experimentally confirmed that branched polyethylene shows cellulation of spherulites due to the segregation of branches in polyethylene chains.[57]

We also suppose another type of fingering instability driven by the difference in densities of the crystal and the liquid. Because of the difference, there must be a flow to supply polymer molecules to the growth front, and the flow must be driven by the gradient of chemical potential. Then, the gradient can be the origin of the branching instability similar to Saffman−Taylor instability[50,51] of so-called "viscous fingering" caused by the mechanical (pressure) gradient in a viscous fluid.

In the following, we present the rough sketch of the branching instability caused by a gradient field. On the basis of the gradient of the chemical potential formed at the growth front of a spherulite (Figure 3), with a small fluctuation of wavenumber, q, of the shape of growing interface, $y(x) = y_0 + A\cos(qx)$, the part sticking out from neighboring area can grow faster because of the gradient giving larger supercooling. On the other hand, the fluctuation gets suppressed by the effect of surface tension, γ. Owing to those two effects, the driving force of the chemical potential difference per segment, $\Delta\mu$, at the growth front is modified from the value at the mean position of y_0, $\Delta\mu_0$, as follows:

$$\Delta\mu(x) \simeq \Delta\mu_0 + a(y - y_0) + v_s\gamma\frac{d^2y}{dx^2} \tag{1}$$

with the gradient, a, and the specific volume of a segment in the crystal, v_s. We suppose that the growth rate is basically limited by surface nucleation process on the basis of the standard model of Lauritzen and Hoffman.[58] The second and the third terms on the right-hand side of eq 1 act as small perturbations of the linear growth rate, $V(\Delta\mu_0/k_BT)$, determined by the driving force at the mean position of the interface, $\Delta\mu_0$. For the perturbations small enough, we can have the following expansion of the growth rate

$$V\left(\frac{\Delta\mu(x)}{k_BT}\right) \simeq V\left(\frac{\Delta\mu_0}{k_BT}\right)\left[1 + \frac{C}{k_BT}(a - v_s\gamma q^2)A\cos(qx)\right] \tag{2}$$

with a kinetic coefficient, C, and the Boltzmann constant, k_B, at the crystallization temperature, T.

The balance of the two effects in eq 2 determines the critical wavelength, λ, for the acceleration of fluctuation, i.e., $a - v_s\gamma q^2 > 0$, as follows:

$$\lambda = 2\pi\left(\frac{v_s\gamma}{a}\right)^{1/2} \tag{3}$$

We suppose that the critical wavelength corresponds to the lamellar width just before splaying into branches, i.e., the maximum width at the growth front, λ_m.

Now, the compositional gradient at the growth front moving at the velocity, V, is expressed as[47]

$$c = c_\infty + \Delta c\exp\left[-\frac{y - y_0}{\delta}\right] \tag{4}$$

with the diffusion length, δ, given by the growth rate, V, and the coefficient of interdiffusion, D, as

$$\delta = \frac{D}{V} \tag{5}$$

Here, c represents the volume fraction of the fractions having lower melting points and being rejected at the growth front; c_∞ and Δc are the preset volume fraction and the increase in the fraction accumulated at the growth front, respectively. The increase in chemical potential of Flory–Huggins's type[59] with the change in composition gives the gradient, a, and the critical wavelength, λ, by using eq 3, as follows:

$$a \simeq \frac{\Delta ck_BT}{x_1\delta} \tag{6}$$

$$\lambda \simeq 2\pi\left(\frac{x_1v_s\gamma}{\Delta ck_BT}\delta\right)^{1/2} \tag{7}$$

where x_1 represents the number of segments of the fractions rejected at the growth front.

On the other hand, for the pressure gradient, dp/dy, in the viscous melt, the gradient in chemical potential, a, is determined by the Clausius−Clapeyron relation between pressure and temperature of the melting line and will be given as

$$a = \Delta v\frac{dp}{dy} \tag{8}$$

with the difference in the specific volume of a segment between the crystal and the melt, Δv. In the fluid of viscosity, η, the pressure gradient induces the shear flow of thickness, b, with the flow rate, v, being proportional to the gradient as $v = b^2(dp/dy)/(12\eta)$.[51] The flow rate to balance the density difference will be given as $v = V\Delta v/v_s$, and hence the critical wavelength is expressed as

$$\lambda' = 2\pi b\frac{v_s}{\Delta v}\left(\frac{\gamma}{12V\eta}\right)^{1/2} \tag{9}$$

Ring Periodicity, *P*. In the above modeling of the consecutive branching and twisting reorientation of branches, those lamellar crystallites will eventually evolve a macroscopic twist along the radial direction (Figure 2b). Considering the contributions of both of continuous twist with a coefficient, t, representing the length along the radial direction required for the lamellar twist of unit radian and of the angle of reorientation on the occasion of splaying, $\Delta\theta$, the following relation will hold for the ring period, P, and the mean distance between successive branching, Λ:

$$\pi = \frac{P}{t} + \Delta\theta\frac{P}{\Lambda} \tag{10}$$

Here, the length, Λ, represents the length of each branch grown in the time interval between the repeated branching, while in the same time interval the width reaches the maximum width, λ_m, at which the growth face becomes unstable. By simple geometrical consideration, the ratio, g, of λ_m and Λ is determined by the axial ratio of growth rates and will be of the order of

one for polyethylene grown from the melt.[27] The expression of the ring period, P, in terms of λ_m will then be given as follows:

$$P = \frac{\pi}{1/t + \Delta\theta/g\lambda_m} \tag{11}$$

In this expression, if the reorientation on the occasion of splaying is dominant in comparison with the continuous lamellar twist in a banded spherulite, i.e., $\Delta\theta/g\lambda_m \gg 1/t$, the ring period, P, will be proportional to the lateral size of lamellae, λ_m.

For the proportional relationship between P and λ_m, there can be another possibility that the pitch of continuous twist is limited by the lateral size, as recently suggested by Muthukumar in his theoretical modeling,[42] so that the coefficient, t, is also in proportion to λ_m. In this case, the proportional dependence of P on λ_m is also expected for the continuous twist without the dominant contribution of the reorientation on splaying. For this reason, in the present modeling, we have the following final form of the expression, and we just suppose the proportional dependence irrespective of the cause of the relationship

$$P = \frac{\pi g'}{\Delta\theta}\lambda_m \tag{12}$$

where the coefficient, $g'/\Delta\theta$, includes the contributions of both the amplified twist on splaying and the continuous twist limited by the lamellar width. We think it will not be unrealistic to suppose the correlation between the periodicity in the higher order structure and the size of the building blocks, i.e., the lateral size of the lamellar crystals.

It is noted that the present modeling predicts the coupling of the band spacing and the physical gradient at the growth front. An approach to the origin of continuous twist based on a similar coupling has been proposed by Schultz.[60] He supposed the gradient field in the direction normal to the basal surfaces of lamellae to induce torsional deformation in the lamellar crystal. For the justification of the modeling, there must be inherent torsional surface stresses in order to cause the torsional deformation rather than scrolling and to select the handedness of the torsion because the self-created field does not spontaneously choose the torsion with one of the handedness from other possible deformations. For this reason, we think that the modeling of Schultz will be considered as a possible intensifying effect on the continuous twist basically caused by the inherent torsional surface stresses. We also suppose that the same will apply to the theoretical modeling of rhythmic banding in a spherulite based on the coupling of compositional and orientational orders.[61]

From the above expressions, the dependence on the growth condition of the ring period, P, and the maximum width, λ_m, is summarized as

$$P \propto \lambda_m \propto \left(\frac{D}{V}\right)^{1/2} \quad \text{or} \quad \left(\frac{1}{V\eta}\right)^{1/2} \tag{13}$$

for compositional gradient or for mechanical (pressure) gradient, respectively, under the assumption that the changes in other factors, $\Delta\theta$, g', and γ, are weak enough. In the following experiments, we will examine this relationship between the growth rate, V, the maximum lamellar width at the growth front, λ_m, and the ring period, P.

Experimental Section

Polyethylene was NIST SRM 1482 of M_w =13 600 and M_w/M_n = 1.19 (PE14K), NIST SRM 1483 of M_w = 32 100 and M_w/M_n = 1.11 (PE32K), and NIST SRM 1484 of M_w = 119 600 and M_w/M_n = 1.19 (PE120K). For the crystallization from the melt, a film of several micrometers thick was prepared on a cover glass by solution casting, melted at 160 °C for 2 min, and crystallized isothermally at 110−121 °C. By sliding the cover glass between two hot cells kept at the melting and crystallization temperature, the isothermal crystallization was achieved after about 1 s,[55] so that we could examine the crystallization at much lower temperature than with a conventional hot stage for optical microscopy. After the isothermal crystallization for a certain time interval, the sample was quenched in a freezing acetone (∼−90 °C) or isopentane (∼−160 °C) by dropping the cover glass from the crystallization cell. Owing to the thin sample thickness (∼ several micrometers), the quench was almost instantaneous. The spherulites were examined with a polarizing optical microscope, POM (BX51, Olympus Corp.), for the measurements of the ring period and the growth rate from the change in size with crystallization time.

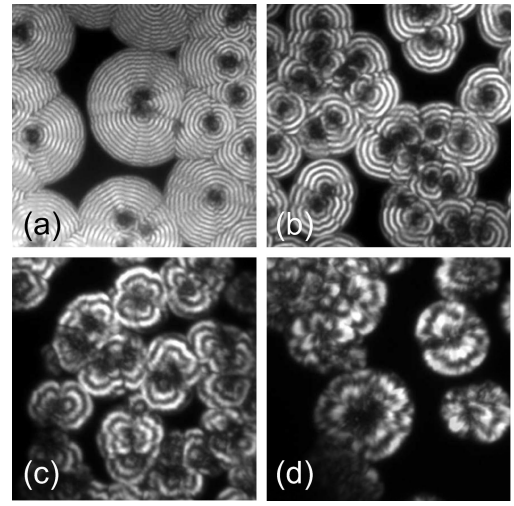

Figure 4. 100 × 100 μm^2 POM images of PE ringed spherulites of 32K fraction grown from the melt at (a) 112, (b) 114, (c) 116, and (d) 118 °C. In order to eliminate the Maltese cross of spherulites, two images of the same area differing the polarization direction by 45° are superimposed.

For the microscopic examination of lamellar crystals at the growth front of spherulites, we need to remove surrounding microcrystallites and amorphous portions formed on quenching. For this purpose, the samples were subsequently subjected to permanganic etching.[62] The samples were then examined with an atomic force microscope, AFM (SPI3800N, Seiko Instruments Inc.), in a dynamic force mode in air. Silicon cantilevers (SI-DF20, Seiko Instruments Inc.) with a resonance frequency of 110–150 kHz were used for the observations. By AFM, we have measured the lateral width of crystals at the growth front of spherulites and supposed that the maximum size corresponds to the critical width for the onset of branching; we have averaged the size of several large crystals as typically shown in Figure 5 by two-headed arrows.

Results and Discussion

Figures 4 and 5 show the POM images of PE spherulites of 32K fraction and the AFM images of lamellar crystals at the growth front crystallized at the respective temperatures. It is evidently seen that both the ring period and the lateral width of crystals undergo consistent changes with crystallization temperatures. Similar changes have also been confirmed for the 120K fraction (Figure 6). For the 14K fraction, there were no rings in the spherulites obtained under isothermal conditions, and the lamellar crystals were quite wide in comparison with those in higher molecular weight fractions, as shown in Figure 7.

Figure 8a shows the growth rate, V, divided by the temperature dependence of Vogel−Fulcher type, D_T, of mass diffusion coefficient represented as

$$D_T \equiv \frac{D}{D_0} = \exp\left[-\frac{B'}{T - T_0}\right] \tag{14}$$

where D_0 is a coefficient depending on molecular weight and B' = 1200 K and T_0 = −100 °C are the coefficients of the

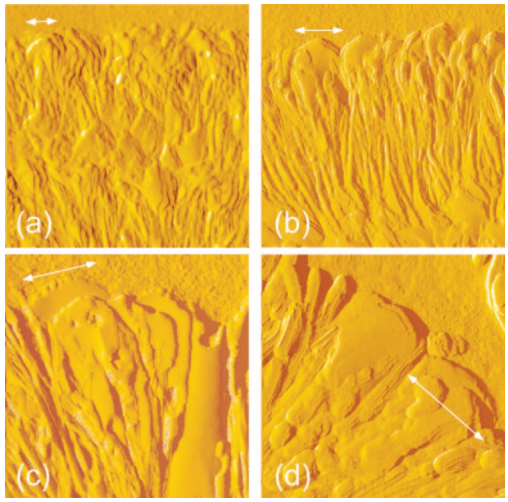

Figure 5. 3 × 3 μm^2 AFM amplitude images near the growth front of polyethylene spherulites of 32K fraction grown from the melt at (a) 111.3, (b) 113.8, (c) 116.3, and (d) 117.6 °C.

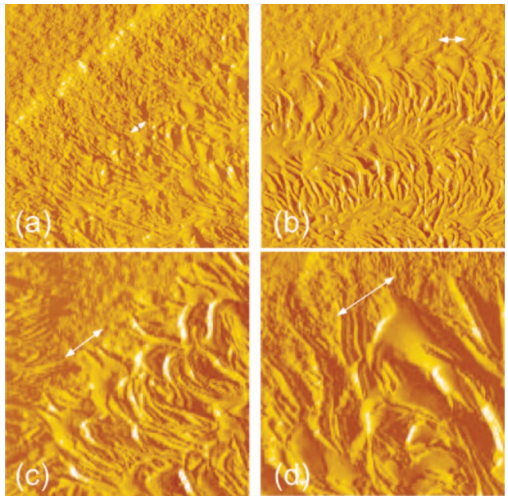

Figure 6. 5 × 5 μm^2 AFM amplitude images of 120K fraction at (a) 112.0, (b) 114.0, (c) 116.0, and (d) 120.0 °C.

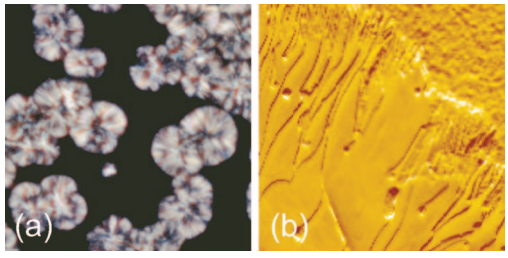

Figure 7. (a) 100 × 100 μm^2 POM and (b) 6 × 6 μm^2 AFM amplitude images of 14K fraction crystallized at 116 °C.

Vogel−Fulcher type for polyethylene.[63] Owing to Einstein's relation, η^{-1} in eq 13 has the same temperature dependence as D, and hence the plots of VD_T^{-1} in Figure 8a have the same meaning as those of $V\eta_T$. It also needs to be mentioned that, in a practical sense, the temperature dependence of eq 14 only has a minor effect for such a narrow temperature range shown in Figure 8.

Figure 8b,c shows the logarithmic plots of the lateral width of crystallites at the growth front, λ_m, and the ring period, P. As seen in Figure 8, because of the narrow temperature range, the data points can be fitted by straight lines, and the ratio of the slopes of log VD_T^{-1} and log λ_m is close to −2:1 for the

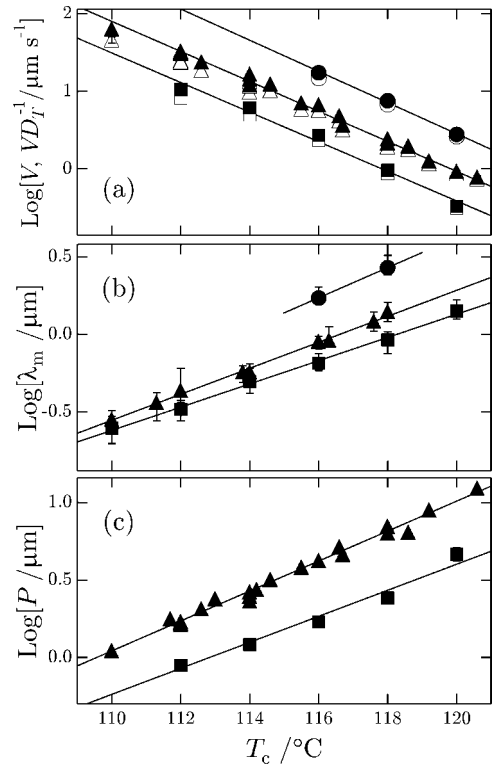

Figure 8. Logarithmic plots of (a) V (open) and VD_T^{-1} (filled), (b) λ_m, and (c) P against crystallization temperature. Symbols represent the results of 14K (●), 32K (▲), and 120K (■) fractions. The slopes of fitting lines are (a) –0.20, –0.19, –0.19 and (b) 0.098, 0.084, 0.075 for 14K, 32K, and 120K fractions and (c) 0.097, 0.084 for 32K and 120K fractions, respectively. VD_T^{-1} in (a) is divided by a constant, 220, to overlap with V.

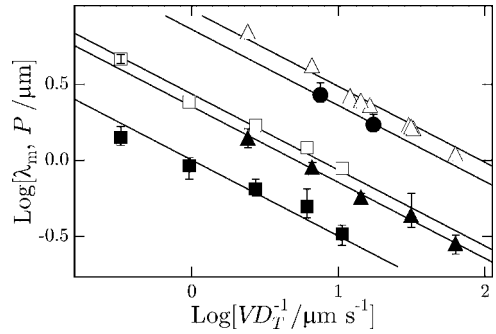

Figure 9. Double-logarithmic plots of λ_m (filled) and P (open) against VD_T^{-1} for 14K (●), 32K (▲, △), and 120K (■, □) fractions. The slopes of all straight lines are –0.5.

fractions. The ratio of the slopes of log λ_m and log P is close to 1:1 for the fractions of 32K and 120K having banded spherulites. The double-logarithmic plots in Figure 9 also suggest the relationship directly; the slope of −0.5 indicates the predicted dependences and the data points are on the fitting straight lines. Therefore, Figures 8 and 9 confirm the expected relationship of eq 13.

The proportional relationship between the band period, P, and the maximum lateral width, λ_m, suggests the strong correlation between them. There are two possibilities for the relationship, as suggested in the above: the amplified twist on splaying and the continuous twist limited by the lamellar width. On the other hand, the square root dependence of λ_m and P on VD_T^{-1} (or $V\eta_T$) suggests the branching instability due to a gradient in chemical potential at the growth front. For the successful confirmation of those relationships, the examination

of the width at the growth front must be essential; the width behind the growth front becomes wider on crystallization, as indicated in Figure 2b, until the impingement on other lamellae, and hence does not correspond to the critical width.

An additional examination can be made on the quantitative examination of the critical width expressed as eqs 7 and 9. For polyethylene, we know the self-diffusion coefficient, D, experimentally determined as the following expression in terms of the weight-averaged molecular weight, M_w: $D = 1.7 \times 10^{-8} M_w^{-2}$ μm^2/s at 175 °C for M_w = 600–120 000 determined by NMR.[63] At 118 °C, eq 14 gives $D = 0.6 \times 10^{-8} M_w^{-2}$ μm^2/s. On the other hand, the growth rate of the 32K fraction was $V \simeq 2$ μm/s at 118 °C, and hence the mass diffusion length for the compositional gradient, δ, at 118 °C is estimated to be $D = 3 \times 10^7 M_w^{-2}$ μm. For the average molecular weight of 32K fraction, δ is then estimated as $\delta \simeq 0.03$ μm. The evaluated mass diffusion length is much shorter than the thermal diffusion length, δ_{th}, which is much larger than the size of spherulites; $\delta_{th} \sim 0.3$ m is estimated from $V = 2$ μm/s and the thermal diffusivity, $D_{th} \sim 3 \times 10^5$ μm^{-2}/s.[64] Such small value of the mass diffusion length indicates steep compositional gradient at the growth front and supports the possibility of the instability due to compositional gradient. The other factors in eq 7 for the compositional gradient can be evaluated from literature values, as $\gamma \simeq 10$ erg/cm^2,[58] $k_B T \simeq 5.4 \times 10^{-14}$ erg at 118 °C, $x_1 \nu_s = M_1/\rho N_A \simeq 1.7 \times 10^{-24} M_1$ cm^3 with the density $\rho \simeq 1$ g/cm^3, the Avogadro number N_A, and the molecular weight M_1 of the fraction rejected at the growth front. Then, the observed lamellar width of $\lambda_m = 1.3$ μm at 118 °C can be predicted for $M_1/\Delta C = 5 \times 10^5$ g/mol by using eq 7. If we choose the molecular weight, M_1, lower than the average, e.g., $M_1 = 10^4$ g/mol, the condition means $\Delta C = 0.02$, which will not be unrealistic even for the fractionated polymer.

For the possibility of pressure gradient, the viscosity, η, is estimated as $\eta = 10^{-13} M_w^{3.6} P$ at 118 °C from the value $\eta = 3.8 \times 10^{-14} M_w^{3.6} P$ at 175 °C for $M_w > 5000$[63] by using eq 14. Another factor, $v_s/\Delta v$, in eq 9 is expressed as $v_s/\Delta v = \rho_{cryst}^{-1}/(\rho_{melt}^{-1} - \rho_{cryst}^{-1}) = 0.97^{-1}/(0.80^{-1} - 0.97^{-1}) \simeq 4.7$ at 118 °C,[65,66] and hence, for $\lambda_m = 1.3$ μm at 118 °C, the thickness of shear flow, $b \simeq 0.03$ μm, is estimated from eq 9. The estimated thickness is much thinner than the film thickness of several micrometers. This estimate will not be unrealistic if we suppose that the thickness, b, does not correspond to the thickness of the melt film but to that of the bundle of lamellae.

The judgment of the applicability of compositional gradient and/or pressure gradient will be difficult only from the evaluation of the accumulated volume fraction, Δc, for the compositional gradient and the thickness of shear flow, b, for the pressure gradient. In the present experiments with different molecular weight fractions, we can also examine the molecular weight dependence. The molecular weight dependence of diffusion coefficient in eq 7 is expressed as $D \propto M_w^{-2}$ and that of viscosity in eq 9 as $\eta \propto M_w^{3.6}$.[63] Therefore, for the compositional gradient, due to the dependence of D and that of x_1 in eq 7, the molecular weight dependence of the product of $\lambda_m^2 V D_T^{-1}$ will be represented as

$$\lambda_m^2 V D_T^{-1} \propto x_1 D_0 \propto M_w^{y-2}, \quad 0 \le y \le 1 \tag{15}$$

The power, y, is determined by the change of the molecular weight, x_1, of the fraction rejected at the growth front for the respective M_w. On the other hand, for pressure gradient of eq 9, we suppose that similar product, $\lambda_m^2 V \eta_T$, will have the power of 3.6 due to the molecular weight dependence of η_0. Figure 10 shows the product for 14K, 32K, and 120K fractions, and Figure 11 shows the logarithmic plots of the molecular weight dependence of $\lambda_m^2 V D_T^{-1}$ (or of corresponding $\lambda_m^2 V \eta_T$). The slope of the plot in Figure 11 indicates the dependence

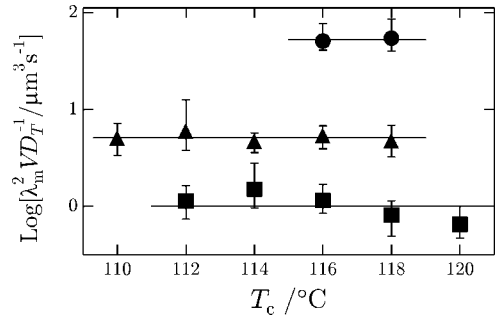

Figure 10. Plots of $\lambda_m^2 V D_T^{-1}$ against crystallization temperature. Symbols represent the results of 14K (●), 32K (▲), and 120K (■) fractions.

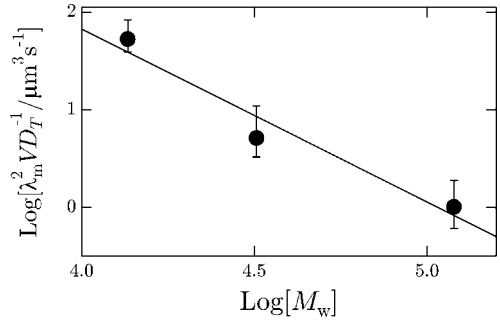

Figure 11. Double-logarithmic plots of the mean value of $\lambda_m V D_T^{-1}$ in Figure 10 against M_w.

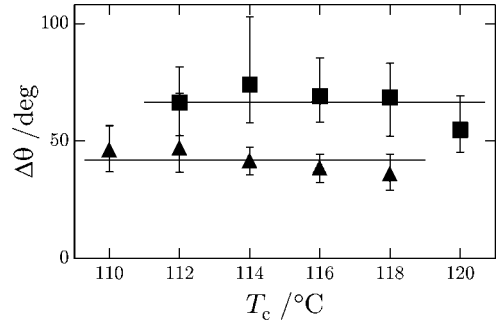

Figure 12. Plots of $\Delta\theta$ against crystallization temperature. Symbols represent the results of 32K (▲) and 120K (■) fractions.

proportional to $M_w^{-1.8}$, which is in the range expected for the compositional gradient of eq 15. Therefore, the molecular weight dependence seems to support the possibility of compositional gradient as the origin of the gradient field. However, we should be cautious about making conclusion on this point because of very thin thickness (~ 0.03 μm) expected for the shear flow. If the transportation of chains at the growth front is dominated by the mode of reeling-in of chains, the effective viscosity will be in proportion to M^1 and have much weaker dependence on molecular weight. For those reasons, it will be safe to state that the mechanisms of both compositional gradient and pressure gradient are not excluded by the present experimental results.

Effects of Lamellar Thickness. In the present modeling, we have supposed the torsional stress at the upper and lower surface regions of lamellar crystals with chain folding.[12] For this reason, on the basis of eq 12, we expect a tendency of smaller angle, $\Delta\theta$, for thicker lamellae being less susceptible to twist. We also expect larger $\Delta\theta$ for higher molecular weight fraction due to higher degree of congestion with longer cilia and tie chains in the folding region. Figure 12 shows $\Delta\theta$ estimated from the ratio of λ_m/P by using eq 12 under the assumption of $g' \simeq 1$. In Figure 12, we can confirm both the expected tendencies of

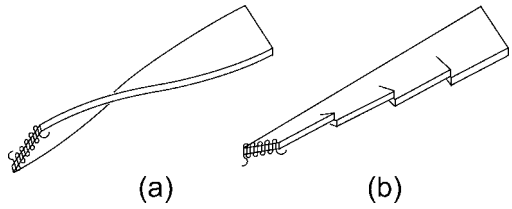

Figure 13. Schematic illustrations of possible modes of twist with intrinsic torsional stress: (a) continuous twist and (b) sequential creation of axial screw dislocations of the same handedness.

smaller $\Delta\theta$ for thicker lamellae at higher temperatures and larger $\Delta\theta$ for higher molecular weight.

Besides the effect on $\Delta\theta$ of lamellar thickness in the present modeling, historically well-known approaches to the ring periodicity predict the dependence of the pitch of twist on lamellar thickness based upon the expectation for thinner lamellae being more susceptible to twist. With the intrinsic torsional stress inherent in the folding surfaces of thin lamellar crystallites, the periodicity has been explained mainly by the following two possible mechanisms (Figure 13): continuous lamellar twist[67,68] and sequential creation of axial screw dislocations of the same handedness.[69]

First, in terms of the continuous lamellar twist due to inherent stress in the surface regions, it has been predicted that the pure torsion brings the period of rings, P_1, given as follows[68]

$$P_1 = \frac{\pi}{6}\left(\frac{G}{\gamma_e \delta}\right)\ell^2 \tag{16}$$

where G represents the elastic modulus, γ_e an excess surface tension due to the inherent stress, and δ the thickness of the surface regions.

On the other hand, an axial screw dislocation is expected to cause twisting, as is the case of Eshelby's twist.[70] Then, the sequential creation of screw dislocations of the same handedness will evolve macroscopic twist (Figure 13b). If the dislocations are created by thermal fluctuations, the ring period, P_2, will be determined by the creation probability which is exponentially dependent on the strain energy in proportion to ℓ^3. Then, the dependence on ℓ of P_2 will be given as[69]

$$P_2 \propto \exp\left[\frac{C_{dis}\ell^3}{k_B T}\right] \tag{17}$$

where C_{dis} is the coefficient derived from the elastic modulus of crystals for the creation energy of the dislocation. For polyethylene crystal, the coefficient, C_{dis}, is given as

$$C_{dis} = \frac{K}{4\pi}\ln\left[\frac{R}{r_0}\right] \tag{18}$$

where the constant, K, is determined by the elastic modulus of polyethylene crystal[71] and is estimated as $K = 1.5 \times 10^9$ J/m^3 for the screw dislocation of the Burgers vector in the thickness direction. On the other hand, R and r_0 in eq 18 represent the size of the area undergoing the elastic deformation and that of dislocation core, respectively. Because of the logarithmic dependence, the factor $\ln[R/r_0]$ contributes to the evaluation of C_{dis} only as a factor less than 10. Consequently, the coefficient is estimated as $C_{dis} \geq 10^8$ J/m^3.

Figure 14 shows the results of our observations of 32K fraction of polyethylene spherulites on the ring period, P, plotted against the lamellar thickness, ℓ, evaluated for the same fraction grown from the melt by Barham et al.[72] As shown in Figure 14a, the dependence of P on ℓ cannot be fitted by a parabolic curve at all and shows much stronger dependence with the power of 9.2. The relationship can also be fitted by an exponential dependence in Figure 14b. The dependence seemingly supports

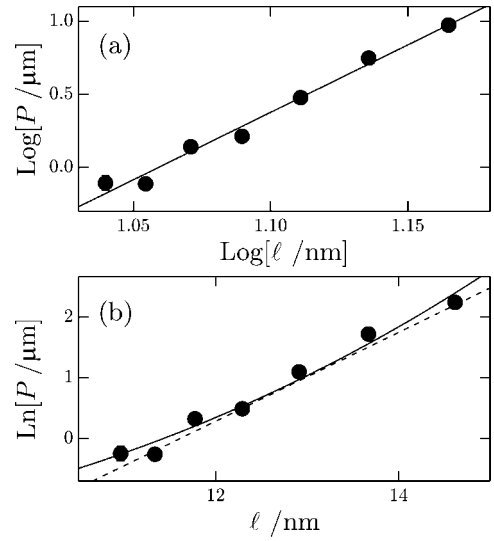

Figure 14. Plots of the ring period of polyethylene spherulites against lamellar thickness: (a) double-logarithmic and (b) semilogarithmic plots. The solid line in (a) represents $P \propto \ell^{9.2}$ and in (b) $P \propto \exp[C_{exp}\ell^3/k_B T]$ with $C_{exp} = 8 \times 10^3$ J/m^3. The broken line in (b) represents the linear relationship expected from the experimental data of P, V, and ℓ on the basis of the present modeling.

the mechanism based on the thermal creation of growth dislocations represented by eq 17. However, the quantitative examination of the activation energy indicates serious disagreement. The coefficient of the fitting in Figure 14b by eq 17, $C_{exp} = 8 \times 10^3$ J/m^3, is smaller than the calculated value by 4 orders of magnitude. The evaluation of the dislocation energy with $C_{dis}\ell^3$ in eq 17 may overestimate the energy of giant screw dislocation, supposing linear elastic strain energy for a displacement of magnitude, ℓ, larger than 10 nm. Keith and Padden[23] estimated the energy required for the vertical shift of one end of a 0.3×0.3 μm^2 lamella of polyethylene by 10 nm to be about 6×10^{-19} J, while $C_{exp}\ell^3$ in Figure 14b gives 8×10^{-21} J for $\ell = 10$ nm. The discrepancy is now 2 orders of magnitude. We think that the discrepancy is quite large in both evaluations and suggests almost perfect compensation of the strain energy of dislocation by that of intrinsic strain, which will be quite unlikely.

In this way, both of the approaches based on the effect of lamellar thickness are unsuccessful in the explanation of the systematic change in the ring period of polyethylene spherulites. It is noted that similar behavior of the thickness dependence of ring period can be read from the reported results on poly(3-hydroxybutyrate).[73] It is therefore suggested that the determining factor of the period of bands is not the lamellar thickness but the lateral width of lamellae in the form of the proportional dependence, as shown above.

In terms of the thickness dependence, on the basis of the present modeling, an exponential dependence of P on ℓ is predicted because of the relationship of $P \propto (D/V)^{0.5}$ and the well-known linear relationship of $\ln[D/V]$ and ℓ both depending linearly on $1/\Delta T$.[58] Then, the present modeling gives the linear relationship shown in Figure 14b as the straight broken line. We think the agreement is good enough.

Other Polymer Spherulites. Regarding the applicability of the present modeling to other polymer banded spherulites, we have experimentally confirmed the relationship of $P \propto \lambda_m \propto (D/V)^{1/2}$ for poly(vinylidene fluoride) grown from the melt.[74] For poly(3-hydroxybutyrate),[73] *cis*-1,4-polybutadiene,[75] and poly(L-lactic acid),[76] the relationship of $P \propto (D/V)^{\alpha}$ with $\alpha \sim 0.5$ can be read from the existing reports, if we take account of the temperature dependence of D of WLF type. For those

polymers, the experimental examination of λ_m will be required. It should also be noted that we do not intend to generalize the present argument to all banded spherulites of polymers. For the banded spherulites of poly(L-lactic acid)[76] and poly(ϵ-caprolactone)[77] grown from the blends with miscible polymers, not only the segregation effect of miscible polymers but also the direct interaction of miscible polymers with the lamellar surfaces seems to be an important factor for the period determination probably due to more unbalanced surface stresses by the physical adsorption of the miscible polymers. For the banded spherulites formed by monodisperse long paraffin,[78] we have to exclude the possibility of compositional gradient; the stress caused by surface reorganization with thickening and/or ciliation[5] may be coupled with pressure gradient to cause the instability.

Concerning the general formation mechanism of polymer spherulites including nonbanded spherulites, the present modeling and the experimental results of banded polyethylene spherulites strongly suggest the possibility of the instability of growth front caused by a gradient in chemical potential for the branching mechanism of lamellar crystallites. In a recent work of Gránásy et al.,[79] they have suggested the role of dynamic heterogeneities caused by the decoupling of translational diffusion from orientational relaxation as the source of grain nucleation at the growth front for the formation of spherulites at temperatures, T_c, near the glass transition, T_g, i.e., $T_c \leq 1.2T_g$. Concerned with polymer spherulites, it is known that the spherulites are formed at temperatures much higher than $1.2T_g$, and hence they have supposed that a fixed angle of misorientation of splaying plays a crucial role for the formation.[80]

We suppose that the reorientation on the occasion of splaying can be the source of this type of misorientation of splaying. Even for nonbanded spherulites, we expect an excess surface stress caused by the folding of chains, though the stress will be inhomogeneous and will not have consistent torsional component; the stress will lead to random reorientation of twist on splaying. Random reorientation will also be caused the pressure from uncrystallized molecular portions of cilia confined between lamellae, as has been proposed by Bassett and Olley[43] for nonbanded spherulites. We have recently confirmed that the correlation length of lamellar orientation in the nonbanded spherulites of poly(butene-1) in form II follows the dependence expected for the random reorientation of branching.[81]

Conclusion

In the present paper, we have examined the correlation between the sharp variation of the periodicity of extinction rings in polyethylene banded spherulite and the variations in the lamellar width and the growth rate. We have experimentally examined those factors by optical and atomic force microscopies for three different molecular weight fractions of polyethylene at relatively low crystallization temperatures where the band spacing shows a sharp variation by almost 1 order of magnitude. The obtained results for the fractions satisfied the relationship of eq 13, namely the proportional relationship between the band spacing and the lamellar width and the square root dependence on the growth rate of those characteristic lengths.

The proportional relation between the band spacing and the lamellar width suggests the strong correlation, which can be due to nonuniform twist amplified on splaying or due to continuous twist limited by the lateral size of lamellae. The square root dependence of the band spacing and the lamellar width on the growth rate indicates that those characteristic lengths are determined by the branching instability induced by a gradient field. A typical example of tip splitting due to branching instability has been observed for a polyethylene crystal formed on the course of quenching (Figure 1).

For those behaviors, we have suggested a mechanism incorporating the branching instability at the growth front and the spontaneous twist by surface stresses (Figure 2); both of the elements have been discussed in detail in prior studies, but the coupling of them has not been considered before. Branching and the subsequent reorientation due to the inherent stress will result in the repetition of branching and twisting reorientation of individual crystallites at the growth front. The modeling has common features with the morphological observations of the repetitive lamellar twisting and splaying in a banded spherulite confirmed by Briber and Khoury[41] and the branching and splaying of individual dominant lamellae confirmed by Bassett et al.[40,43,44] We have provided the model based on the above-mentioned experimental evidence and examined the applicability in a quantitative manner especially in relation with the periodicity of rings and with the branching instability. We think that the present results of the banded spherulites also suggest possible important role of branching instability of growth front for the formation of polymer spherulites in general.

We have supposed that the branching instability is caused by the gradient in chemical potential at the growth front. We considered the possibilities of compositional gradient similar to the Mullins−Sekerka type of cellular instability[48,49] and mechanical (pressure) gradient similar to the Saffman−Taylor type of viscous fingering,[50,51] both of which predict the square root dependence on the growth rate of the maximum lateral width of lamellar crystals at the growth front, as in eq 13. The identification of the gradient field including other possibilities will need more experimental and theoretical examinations and will be a quite important issue to be clarified in our future work.

Acknowledgment. The authors thank Dr. M. Nonomura and Prof. S. Tanaka of Hiroshima University, Prof. Y. Yamazaki of Waseda University, and Prof. T. Taniguchi of Yamagata University for helpful discussions and acknowledge the valuable discussions at the Yukawa Institute for Theoretical Physics (YITP-W-05-04). This work was partially supported by MEXT Japan, Grant-in-Aid for Scientific Research on Priority Areas, "Creation of Nonequilibrium Soft Matter Physics".

References and Notes

(1) Bernauer, F. *Gedrillte Kristalle*; Borntraeger: Berlin, 1929.
(2) Keller, A. *Nature (London)* **1952**, *169*, 913.
(3) Geil, P. H. *Polymer Single Crystals*; John Wiley: New York, 1963.
(4) Magill, J. H. *J. Mater. Sci.* **2001**, *36*, 3143.
(5) Bassett, D. C. *J. Macromol. Sci.* **2003**, *B42*, 227.
(6) Point, J. J. *Bull. Acad. R. Bel.* **1953**, *41*, 982.
(7) Keith, H. D., Jr *J. Polym. Sci.* **1959**, *39*, 123.
(8) Price, F. P. *J. Polym. Sci.* **1959**, *39*, 139.
(9) Keller, A. *J. Polym. Sci.* **1959**, *39*, 151.
(10) Fujiwara, Y. *J. Appl. Polym. Sci.* **1960**, *4*, 10.
(11) Frank, F. C. *Discuss. Faraday Soc.* **1979**, *68*, 7.
(12) Lotz, B.; Cheng, S. Z. D. *Polymer* **2005**, *46*, 577.
(13) Holland, V. F.; Miller, R. L. *J. Appl. Phys.* **1964**, *35*, 3241.
(14) Lotz, B.; Cheng, S. Z. D. *Polymer* **2006**, *47*, 3267.
(15) Geil, P. H. *J. Polym. Sci.* **1960**, *44*, 449.
(16) Cai, W.; Li, C. Y.; Li, L.; Lotz, B.; Keating, M.; Marks, D. *Adv. Mater.* **2004**, *16*, 600.
(17) Vaughan, A. S. *J. Mater. Sci.* **1993**, *28*, 1805.
(18) Lotz, B.; Thierry, A.; Schneider, S. *C. R. Acad. Sci.* **1998**, 609.
(19) White, H. M.; Hosier, I. L.; Bassett, D. C. *Macromolecules* **2002**, *35*, 6763.
(20) Bassett, D. C.; Frank, F. C.; Keller, A. *Nature (London)* **1959**, *184*, 810.
(21) Reneker, D. H.; Geil, P. H. *J. Appl. Phys.* **1960**, *31*, 1916.
(22) Keith, H. D., Jr *Polymer* **1984**, *25*, 28.
(23) Keith, H. D., Jr *Macromolecules* **1996**, *25*, 7776.
(24) Keith, H. D. *Polymer* **2001**, *42*, 9987.
(25) Toda, A.; Keller, A. *Colloid Polym. Sci.* **1993**, *271*, 328.
(26) Toda, A.; Arita, T.; Hikosaka, M. *Polymer* **2001**, *42*, 2223.
(27) Toda, A.; Okamura, M.; Hikosaka, M.; Nakagawa, Y. *Polymer* **2005**, *46*, 8708.

(28) Saracovan, J.; Keith, H. D.; Manley, R.St.J.; Brown, G. R. *Macromolecules* **1999**, *32*, 8918.
(29) Owen, A. J. *Polymer* **1997**, *38*, 3705.
(30) Abo el Maaty, M. I.; Bassett, D. C. *Polymer* **2001**, *42*, 4957.
(31) Patel, D.; Bassett, D. C. *Polymer* **2002**, *43*, 3795.
(32) Keller, A.; Sawada, S. *Makromol. Chem.* **1964**, *74*, 190.
(33) Kunz, M.; Dreschler, M.; Möller, S. *Polymer* **1995**, *36*, 1331.
(34) Lotz, B.; Gonthier-Vassal, A.; Brack, A.; Magoshi, J. *J. Mol. Biol.* **1982**, *156*, 345.
(35) Li, C. Y.; Yan, D.; Cheng, S. Z. D.; Bai, F.; He, T.; Chien, L.-C.; Harris, F. W.; Lotz, B. *Macromolecules* **1999**, *32*, 524.
(36) Li, C. Y.; Yan, D.; Cheng, S. Z. D.; Bai, F.; Ge, J. J.; Calhoun, B. H.; He, T.; Chien, L.-C.; Harris, F. W.; Lotz, B. *Phys. Rev.* **1999**, *B60*, 12675.
(37) Li, C. Y.; Cheng, S. Z. D.; Ge, J. J.; Bai, F.; Zhang, J. Z.; Mann, I. K.; Harris, F. W.; Chien, L.-C.; Yan, D.; He, T.; Lotz, B. *Phys. Rev. Lett.* **1999**, *83*, 4558.
(38) Li, C. Y.; Cheng, S. Z. D.; Weng, X.; Ge, J. J.; Bai, F.; Zhang, J. Z.; Calhoun, B. H.; Harris, F. W.; Chien, L.-C.; Lotz, B. *J. Am. Chem. Soc.* **2001**, *123*, 2462.
(39) Xu, J.; Guo, B.-H.; Zhang, Z.-M.; Zhou, J.-J.; Jiang, Y.; Yan, S.; Li, L.; Wu, Q.; Chen, G.-Q.; Schultz, J. M. *Macromolecules* **2004**, *37*, 4118.
(40) Bassett, D. C.; Hodge, A. M. *Proc. R. Soc. London* **1981**, *A377*, 61.
(41) Briber, R. M.; Khoury, F. *J. Polym. Sci., Part B: Polym. Phys.* **1993**, *31*, 1253.
(42) Muthukumar, M. Presented at the 234th ACS National Meeting, Boston, Aug 19–23, **2007**; Paper no. PMSE 455.
(43) Bassett, D. C.; Olley, R. H. *Polymer* **1984**, *25*, 935.
(44) Bassett, D. C.; Vaughan, A. S. *Polymer* **1985**, *26*, 717.
(45) Keith, H. D., Jr *J. Appl. Phys.* **1963**, *34*, 2409.
(46) Keith, H. D., Jr *J. Polym. Sci., Part B: Polym. Phys.* **1987**, *25*, 2371.
(47) Goldenfeld, N. *J. Cryst. Growth* **1987**, *84*, 601.
(48) Mullins, W. W.; Sekerka, R. F. *J. Appl. Phys.* **1963**, *34*, 323.
(49) Langer, J. S. *Rev. Mod. Phys.* **1980**, *52*, 1.
(50) Saffman, P. G.; Taylor, G. I. *Proc. R. Soc. London, Ser. A* **1958**, *245*, 312.
(51) Fields, R. J.; Ashby, M. F. *Philos. Mag.* **1976**, *33*, 33.
(52) Schultz, J. M. *Polymer Crystallization*; Oxford University Press: Oxford, 2001; Chapter 10.
(53) Taguchi, K.; Miyaji, H.; Izumi, K.; Hoshino, A.; Miyamoto, Y.; Kokawa, R. *Polymer* **2001**, *42*, 7443.
(54) Kajioka, H.; Hoshino, A.; Miyamoto, Y.; Toda, A.; Hikosaka, M. *Polymer* **2005**, *46*, 8717.
(55) Toda, A.; Kojima, I.; Hikosaka, M. *Macromolecules* **2008**, *41*, 120.
(56) Hobbs, J. K.; Humphris, A. D. L.; Miles, M. J. *Macromolecules* **2001**, *34*, 5508.
(57) Abo el Maaty, M. I.; Bassett, D. C.; Olley, R. H.; Jääskeläinen, P. *Macromolecules* **1998**, *31*, 7800.
(58) Hoffman, J. D.; Davis, G. T.; Lauritzen, Jr., J. I. *Treatise on Solid State Chemistry*; Plenum Press: New York, 1976; Vol. *3*, Chapter 7.
(59) Flory, P. J. *Principles of Polymer Chemistry*; Cornell University Press: Ithaca, NY, 1953; Chapter 12.
(60) Schultz, J. M. *Polymer* **2003**, *44*, 433.
(61) Kyu, T.; Chiu, H.-W.; Guenthner, A. J.; Okabe, Y.; Saito, H.; Inoue, T. *Phys. Rev. Lett.* **1999**, *83*, 2749.
(62) Olley, R. H.; Hodge, A. M.; Bassett, D. C. *J. Polym. Sci., Polym. Phys.* **1979**, *17*, 627.
(63) Pearson, D. S.; Ver Strate, G.; von Meerwall, E.; Schilling, F. C. *Macromolecules* **1987**, *20*, 1133.
(64) Young, Y. *Physical Properties of Polymers Handbook*; AIP Press: New York, 1996; p 111.
(65) Orwoll, R. A.; Flory, P. J. *J. Am. Chem. Soc.* **1967**, *89*, 6814.
(66) Cole, E. A.; Holmes, D. R. *J. Polym. Sci.* **1960**, *46*, 245.
(67) Hoffman, J. D., Jr. *J. Res. Natl. Bur. Stand.* **1961**, *65A*, 297.
(68) Okano, K. *Jpn. J. Appl. Phys.* **1964**, *3*, 351.
(69) Schultz, J. M.; Kinloch, D. R. *Polymer* **1969**, *10*, 271.
(70) Eshelby, J. D. *J. Appl. Phys.* **1953**, *24*, 176.
(71) Shadrake, L. G.; Guiu, F. *Philos. Mag.* **1976**, *34*, 565.
(72) Barham, P. J.; Chivers, R. A.; Keller, A.; Martinez-Salazar, J.; Organ, S. J. *J. Mater. Sci.* **1985**, *20*, 1625.
(73) Barham, P. J.; Keller, A.; Otun, E. L. *J. Mater. Sci.* **1984**, *19*, 2781.
(74) Toda, A.; Hikosaka, M.; Taguchi, K.; Kajioka, H., submitted for publication.
(75) Cheng, T.-L.; Su, A.-C. *Polymer* **1995**, *36*, 73.
(76) Xua, J.; Guoa, B.-H.; Zhoub, J.-J.; Lib, L.; Wuc, J.; Kowalczuk, M. *Polymer* **2005**, *46*, 9176.
(77) Keith, H. D., Jr.; Russell, T. P. *Macromolecules* **1989**, *22*, 666.
(78) Bassett, D. C.; Olley, R. H.; Sutton, S. J.; Vaughan, A. S. *Macromolecules* **1996**, *29*, 1852.
(79) Gránásy, L.; Pusztai, T.; Börzsönyi, T.; Warren, J. A.; Douglas, J. F. *Nat. Mater.* **2004**, *3*, 645.
(80) Gránásy, L.; Pusztai, T.; Tegze, G.; Warren, J. A.; Douglas, J. F. *Phys Rev. E* **2005**, *72*, 011605.
(81) Kajioka, H.; Hikosaka, M.; Taguchi, K.; Toda, A. *Polymer* **2008**, doi:10.1016/j.polymer.2008.01.066.

MA702267E